

Efficient Soft-Output Guessing for Enhanced Quantum Tanner Code Decoding

Lukas Rapp,^{1,*} Muriel Médard,^{1,†} Eugene Tang,^{2,‡} and Ken R. Duffy^{3,§}

¹*Research Laboratory for Electronics, Massachusetts Institute of Technology, Cambridge, MA, USA*

²*Department of Mathematics & Physics, Northeastern University, Boston, MA, USA*

³*Department of Mathematics & ECE, Northeastern University, Boston, MA, USA*

(Dated: March 20, 2026)

We introduce a generalized low-density parity-check decoding framework for quantum Tanner codes utilizing soft-output guessing random additive noise decoding (SOGRAND). By soft-output decoding entire component codes, we mitigate trapping sets and cycles, resulting in improved convergence. SOGRAND, combined with ordered statistic decoding (OSD) post-processing, outperforms the standard belief propagation plus OSD baseline by up to three orders of magnitude in logical error rate, providing a way forward for scalable decoding of the emerging class of Tanner-code-based quantum codes.

Quantum error correction is an essential component of large-scale quantum computing. Although the surface code [1, 2] has long been the dominant approach to fault tolerance, high-rate quantum low-density parity-check (QLDPC) codes have recently attracted significant attention due to their potential to greatly reduce qubit overhead [3–7]. The discovery of asymptotically good QLDPC codes [8], and the subsequent development of quantum Tanner codes [9], marked a major milestone in efficient quantum error correction. The theoretical promise of quantum Tanner codes has fueled growing interest in finite-length instances suitable for near-term implementation [10–12], but key obstacles remain, foremost among them the problem of efficient decoding.

Practical implementations require real-time decoding that keeps up with the syndrome generation to avoid an exponential data backlog [13]. To date, quantum LDPC (QLDPC) codes have primarily been decoded using belief propagation (BP), the standard decoder for classical low-density parity-check (LDPC) codes [14]. However, BP struggles in the quantum regime, as stabilizers’ commutativity enforces short cycles, and high degeneracy leads to trapping sets, preventing convergence to syndrome-consistent error patterns [15–17]. Fundamentally, BP’s ability to decode accurately is limited because it relies on the local soft-output decoding of weak single-parity-check constraints. Current proposals include an ordered statistics decoding (OSD) post-processing step [18], applied whenever BP fails (BP+OSD). This approach is effective in improving decoding but comes at the cost of a cubic complexity in codelength, and OSD is currently not believed to admit a feasible near-term VLSI implementation [19].

In this letter, we offer an alternative way forward by exploiting the graphical structure of quantum Tanner codes in conjunction with recent developments in classical soft output decoding. Rather than decoding individual constraints, we treat the code as a *generalized* LDPC code [20] and iteratively soft-decode its more powerful component codes. Unlike previous studies with bit-flipping decoding that focus on identifying asymptotic

bounds [21–25], this proposal processes soft messages, a strategy known to outperform bit-flipping in classical LDPC [14]. By replacing single-parity-check updates with joint decoding of multiple constraints, the short cycles and trapping sets are mitigated. The primary challenge lies in efficiently soft-output decoding these component codes. Recent developments in classical decoding have shown that it is possible to extract accurate soft-output from arbitrary component codes via soft-output guessing random additive noise decoding (SOGRAND) [26]. Its practicability has already been demonstrated in the classical context with a taped-out chip [27]. Although originally designed for classical channels with heterogeneous soft reliability as input, we demonstrate its effectiveness with quantum codes and the statistical soft input inherent to the quantum setting.

The proposed decoder is demonstrated to outperform the BP+OSD baseline by up to three orders of magnitude in logical error rate on instances of quantum Tanner codes [12] while significantly accelerating convergence. Even without the computationally expensive OSD post-processing, the decoder essentially matches the performance of the BP+OSD baseline, removing a critical bottleneck towards scalable decoding. As Tanner code-based constructions are central to the recent development of asymptotically good QLDPC codes [8, 9, 28, 29], this approach serves as a powerful alternative foundation for efficient, real-time decoding across a broad class of emerging quantum error-correcting codes.

Stabilizers and noise.—We consider an $[[n, k, d]]$ stabilizer code [30, 31] defined as the joint $+1$ eigenspace of an abelian subgroup $\mathcal{S} \subset \mathcal{P}_n$, where \mathcal{P}_n denotes n -qubit Pauli group and $-I \notin \mathcal{S}$. As exemplars, we focus on Quantum Tanner codes, which are Calderbank-Shor-Steane (CSS) codes. A CSS code is defined by two parity check matrices $H_X \in \mathbb{F}_2^{m_X \times n}$, $H_Z \in \mathbb{F}_2^{m_Z \times n}$, which specify the X and Z stabilizer generators, respectively and satisfy the CSS condition: $H_X H_Z^T = 0$. While our analysis focuses on CSS codes, the proposed decoder naturally extends to any quantum code that admits a suitable generalized LDPC structure. An error

$E = \bigotimes_{i=1}^n X^{e_{X,i}} Z^{e_{Z,i}} \in \mathcal{P}_n$ is represented by a binary vector $\mathbf{e} = (\mathbf{e}_X | \mathbf{e}_Z) \in \mathbb{F}_2^{2n}$, which yields syndrome pairs $\mathbf{s}_X = H_Z \mathbf{e}_X$, and $\mathbf{s}_Z = H_X \mathbf{e}_Z$. The decoder uses \mathbf{s}_X , and \mathbf{s}_Z to estimate the error patterns $\hat{\mathbf{e}} = (\hat{\mathbf{e}}_X | \hat{\mathbf{e}}_Z)$. The correction succeeds if the residual $\mathbf{e} \oplus \hat{\mathbf{e}}$ belongs to the stabilizer group \mathcal{S} .

As a starting point, we consider the standard code capacity setting [32, 33] as in [18], assuming error-free syndrome measurements, and independent and identically distributed qubit errors E_i . For pedagogical simplicity, we first describe decoding assuming independent X and Z errors, before incorporating X/Z correlation. Owing to the symmetry, we focus on the Z -errors decoder. The decoder is initialized with a vector of log-likelihood ratios (LLRs) \mathbf{L}_{ch} that encapsulate a priori beliefs. Given \mathbf{L}_{ch} , the decoder tries to find an error pattern $\hat{\mathbf{e}}_Z$ that maximizes the posterior probability $P(\mathbf{e}_Z = \hat{\mathbf{e}}_Z | \mathbf{s}_Z)$ while satisfying the *syndrome condition*:

$$H_X \hat{\mathbf{e}}_Z = \mathbf{s}_Z. \quad (1)$$

Quantum Tanner codes.—A classical Tanner code [34] is defined by a linear binary component code, represented by a parity check matrix H_c , and a bipartite graph. The graph consists of n *variable nodes* of degree two, associated with the bits, and m *constraint nodes* (see Fig. 1 left side). Each constraint node $j \in [m] = \{1, \dots, m\}$ enforces a local constraint from H_c on its incident variable nodes. Specifically, let $\mathcal{M}(j)$ be an ordering of the edges connected to constraint node j . The local view of a vector \mathbf{x} at j is the subvector $\mathbf{x}^j = (x_i)_{i \in \mathcal{M}(j)}$, where the ordering is defined by $\mathcal{M}(j)$. A string $\mathbf{c} \in \mathbb{F}_2^n$ is a codeword if and only if the local view at every constraint node $j \in [m]$ is a valid component codeword: $H_c \mathbf{c}^j = 0$. As a linear code, a Tanner code is fully characterized by a global parity check matrix H . *Quantum Tanner codes* [9] are CSS codes, where H_X and H_Z are the global parity check matrices of two classical Tanner codes with component parity check matrices H_{X_c}, H_{Z_c} . They are constructed using an expanding left-right Cayley complex [28], with component codes chosen as dual product codes to ensure that the CSS condition is fulfilled.

Decoding quantum LDPC codes.—Since quantum Tanner codes belong to the class of QLDPC codes, i.e., H_X, H_Z are sparse, they can be decoded with BP [14] as demonstrated in Ref. [12]. In this framework, bit beliefs about error pattern are represented as LLRs. After initializing them with \mathbf{L}_{ch} , they are iteratively exchanged between variable and check nodes until Eq. (1) is satisfied or a maximum number of decoding iterations N_{iter} is reached. To mitigate convergence issues inherent to QLDPC codes, BP+OSD [18] uses OSD as a post-processing step if BP fails to converge. Should BP fail, OSD- w reorders bits by decreasing reliability, derived from the BP soft-output, and finds the most reliable information set via Gaussian elimination on H_X . The decoder then explores 2^w candidate patterns by systemati-

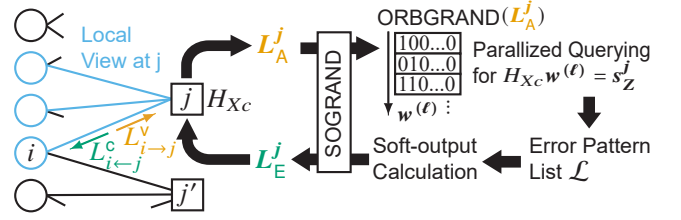


FIG. 1. Overview SOGRAND decoding on generalized LDPC codes. \circ Variable node \square Constraint node. Decoding is performed through iterative message passing on the classical Tanner code (left). During the constraint node update (right), SOGRAND decodes the incoming LLRs \mathbf{L}_A^j and computes extrinsic LLRs \mathbf{L}_E^j . Within this process, SOGRAND identifies a list of likely error patterns that satisfy the local syndrome condition, as well as a likelihood that the correct error pattern has not been identified, from which soft-output is extracted.

cally flipping the w least reliable bits in the information set. For each flipping, the bits outside of the information set are extended to satisfy the syndrome condition, and the pattern with the highest likelihood is selected.

Decoding of generalized LDPC codes.—As quantum Tanner codes are constructed from classical Tanner codes, they are also compatible with iterative decoding techniques originally proposed for their classical counterparts [20, 34]. Instead of treating the Tanner codes as QLDPC codes, we can treat them as *generalized* LDPC codes, leveraging the underlying graph structure, and decode the local views of the component codes rather than weak single-parity-check codes. This approach is made possible by recent advances in classical soft-input soft-output (SISO) decoding of arbitrary multi-bit redundancy codes [26, 35, 36].

To formalize BP under this generalized LDPC interpretation, let $L_{i \rightarrow j}^y, L_{i \leftarrow j}^c \in \mathbb{R}$ be the messages sent from variable node $i \in [n]$ to constraint node $j \in [m_X]$ and from constraint node j to variable node i , respectively (Fig. 1 left).

Init: For each variable node $i \in [n]$, both outgoing messages are initialized as $L_{i \rightarrow j}^y = L_{\text{ch},i}$.

Constraint node update: In parallel, each constraint node $j \in [m_X]$ receives a message vector $\mathbf{L}_A^j \leftarrow (L_{i \rightarrow j}^y)_{i \in \mathcal{M}(j)}$. A SISO decoder takes \mathbf{L}_A^j as soft-input, decodes the local view using the component code H_{X_c} and outputs extrinsic information \mathbf{L}_E^j . These extrinsic LLRs are sent back to the connected variable nodes: $(L_{i \leftarrow j}^c)_{i \in \mathcal{M}(j)} \leftarrow \mathbf{L}_E^j$.

Variable node update: Each variable node $i \in [n]$ receives messages from its two connected constraint nodes $j, j' \in \mathcal{N}(i)$. It calculates the a posteriori probability (APP) LLRs $L_{\text{APP},i} \leftarrow L_{\text{ch}} + L_{i \leftarrow j}^c + L_{i \leftarrow j'}^c$ and hard-decision $\hat{e}_{Z,i}$, which is $\hat{e}_{Z,i} = 0$ if $L_{\text{APP},i} \geq 0$ and 1, otherwise. Finally, it sends the extrinsic messages to both constraint nodes $j \in \mathcal{N}(i)$: $L_{i \rightarrow j}^y \leftarrow L_{\text{APP},i} - L_{i \leftarrow j}^c$.

During each variable node update, the decoder checks whether the current hard-decision $\hat{\mathbf{e}}_Z$ fulfills Eq. (1). If

this is the case or the maximal number of iterations N_{iter} is reached, decoding terminates and $\hat{\mathbf{e}}_{\mathbf{Z}}$ is output.

Soft component decoding.—A central challenge in implementing a generalized LDPC framework for quantum codes is the requirement for an efficient SISO decoder for the component codes. Until recently, there were few practical approaches to SISO decoding of multi-constraint component codes. Most of them require hyperparameters to manage the inability to estimate the likelihood that the true error pattern has not been found. This has changed recently with the establishment of SOGRAND [26], developed from the GRAND methodology [37]. SOGRAND can provide SISO decoding for any moderate-redundancy component code and has been demonstrated in hardware [27], which is why we elect to use it. Recently, the original hard-input, hard-output GRAND framework has been extended to the quantum regime, demonstrating potential for hard-decision decoding of high-rate quantum codes [38–40]. While hard-decision decoding operates without reliability information, we adapt SOGRAND, a more recent and sophisticated SISO version of GRAND. By SISO decoding local component codes, this technique overcomes the rate limitations inherent in previous GRAND-based approaches.

Consider a constraint node $j \in [m_{\mathbf{X}}]$ with parity check matrix $H_{\mathbf{X}_c} \in \mathbb{F}_2^{m_{\mathbf{X}_c} \times n_{\mathbf{X}_c}}$ that receives the soft-input $\mathbf{L}_{\mathbf{A}}^j \in \mathbb{F}_2^{n_{\mathbf{X}_c}}$. We define the *local syndrome* $\mathbf{s}_{\mathbf{Z}}^j = H_{\mathbf{X}_c} \mathbf{e}_{\mathbf{Z}}^j$ at constraint node j as a subvector of the global syndrome $\mathbf{s}_{\mathbf{Z}}$ corresponding to the stabilizers induced by j , where $\mathbf{e}_{\mathbf{Z}}^j$ is the local view of $\mathbf{e}_{\mathbf{Z}}$ at j . To produce accurate soft-output, SOGRAND identifies a list \mathcal{L} of candidate error patterns $\mathbf{w} \in \mathbb{F}_2^{n_{\mathbf{X}_c}}$ that satisfy the local syndrome constraint,

$$H_{\mathbf{X}_c} \mathbf{w} = \mathbf{s}_{\mathbf{Z}}^j, \quad (2)$$

where $\mathbf{L}_{\mathbf{A}}$ determines the a priori probability $P(\mathbf{w}|\mathbf{L}_{\mathbf{A}})$ of each pattern. Since SOGRAND queries noise patterns in approximately decreasing order of likelihood, it ensures that the resulting list contains approximately the most probable syndrome-consistent error pattern.

To achieve this, a noise generator queries patterns $\mathbf{w}^{(1)}, \mathbf{w}^{(2)}, \dots$ in approximately decreasing order of likelihood. Each pattern that satisfies the local syndrome condition in Eq. (2) is added to \mathcal{L} until a maximal list size \mathcal{L}_{max} is reached or a termination condition is met. While noise generators have been proposed for various channels [37, 41, 42], we employ ordered reliability bits guessing random additive noise decoding (ORBGRAND) [41] for its hardware efficiency [43–46].

To extract soft-output from \mathcal{L} , SOGRAND keeps track of the total probability mass P_g of all explored error patterns and of the mass $P_{\mathcal{L}}$ of the patterns in the list \mathcal{L} . Given there are $2^{n_{\mathbf{X}_c} - m_{\mathbf{X}_c}}$ patterns $\mathbf{w}^{(\ell)}$ satisfying Eq. (2) and assuming they are uniformly distributed within the generators’s guessing order, the probability

that a syndrome-consistent error patterns is not in \mathcal{L} can be estimated as $P_{\mathcal{L}^c} = (1 - P_g)2^{-m_{\mathbf{X}_c}}$ [26]. The total syndrome-consistent probability mass $P_{\text{tot}} = P_{\mathcal{L}} + P_{\mathcal{L}^c}$ serves as a normalization factor to calculate APPs conditioned on the local syndrome $\mathbf{s}_{\mathbf{Z}}^j$: $P(\hat{\mathbf{w}}|\mathbf{L}_{\mathbf{A}}, \mathbf{s}_{\mathbf{Z}}^j) \approx P(\hat{\mathbf{w}}|\mathbf{L}_{\mathbf{A}})/P_{\text{tot}}$ for $\hat{\mathbf{w}} \in \mathcal{L}$. This framework enables accurate soft-output estimation by incorporating the uncertainty of the unexplored space when calculating bit-wise marginals \mathbf{L}_{APP} (see Ref. [26] for details). Finally, extrinsic information is computed: $\mathbf{L}_{\mathbf{E}} = \mathbf{L}_{\text{APP}} - \mathbf{L}_{\mathbf{A}}$.

Correlation-aware decoding.—For QLDPCs, X/Z correlation can be incorporated via non-binary BP [15], which was simplified in Ref. [47] to an efficient scalar message-passing scheme. Since quantum Tanner codes are CSS codes with independent X and Z stabilizers, X/Z correlation can also be integrated into the generalized LDPC framework with minimal overhead by decoding X and Z errors simultaneously on their respective classical Tanner codes. This decoder variation can be interpreted as a generalization of Ref. [47] to multi-constraint component codes, applied to CSS codes.

In this case, each variable node $i \in [n]$ is connected to two constraint nodes from each Tanner code, allowing the fusion of incoming beliefs from both subgraphs. To fuse beliefs, we transform each incoming LLR, $L_{i \leftarrow j}^c$, into beliefs $P_{i \leftarrow j}^{c, \mu}$ for all four Pauli operators $\mu \in \mathcal{P} = \{I, X, Y, Z\}$. This is done by accounting for the fact that messages from H_Z and H_X carry no information about Z - or X -errors, respectively. For example, for an incoming message from H_Z , the mapping is: $P_{i \leftarrow j}^{c, X} = P_{i \leftarrow j}^{c, Y} = 0.5q$ and $P_{i \leftarrow j}^{c, I} = P_{i \leftarrow j}^{c, Z} = 0.5(1 - q)$, where $q = (1 + \exp(L_{i \leftarrow j}^c))^{-1}$ is the corresponding bit flip probability. APPs are obtained by normalizing the product of the channel prior $\mathbf{P}_{\text{ch}}^{\mu}$ and all incoming symbol beliefs: $P_{\text{APP}, i}^{\mu} \propto P_{\text{ch}, i}^{\mu} \prod_{j \in \mathcal{N}(i)} P_{i \leftarrow j}^{c, \mu}$. Extrinsic messages are computed by excluding the respective incoming message from the product: $P_{i \rightarrow j}^{v, \mu} \propto P_{\text{APP}, i}^{\mu} / P_{i \leftarrow j}^{c, \mu}$. Finally, these are marginalized back to bit and phase-flip LLRs messages and passed to the constraint nodes.

We note that, as the correlation-aware variant can be interpreted as a generalization of Ref. [47], the proposed framework can be extended to any quantum code with local component codes, including non-CSS codes. Assuming a general component code $\tilde{H}_c \in \mathcal{P}^{m_c \times n_c}$, Eq. (2) becomes $\mathbf{s}_t^j = \bigoplus_{i=1}^{n_c} \tilde{H}_{c, t, i} * \tilde{W}_i$, for $t \in [m_c]$ and $\mathbf{s}^j \in \mathbb{F}_2^{m_c}$. Here, $\tilde{W} \in \mathcal{P}^{n_c}$ is a general error pattern and $\tilde{H}_{t, i} * \tilde{W}_i$ is the symplectic product, which is 0 if $\tilde{H}_{t, i}, \tilde{W}_i$ commute and 1 otherwise. Analogous to Eq. (2), this equation represents a sum of binary variables. A generalized version of the proposed decoder simply passes beliefs about $\tilde{H}_{t, i} * \tilde{W}_i$ along the edges [47], decoding binary component codes, which leaves SOGRAND component decoding completely unchanged.

Results.—We evaluate the performance of SOGRAND decoding on the quantum Tanner codes [[200, 10, 10]] and

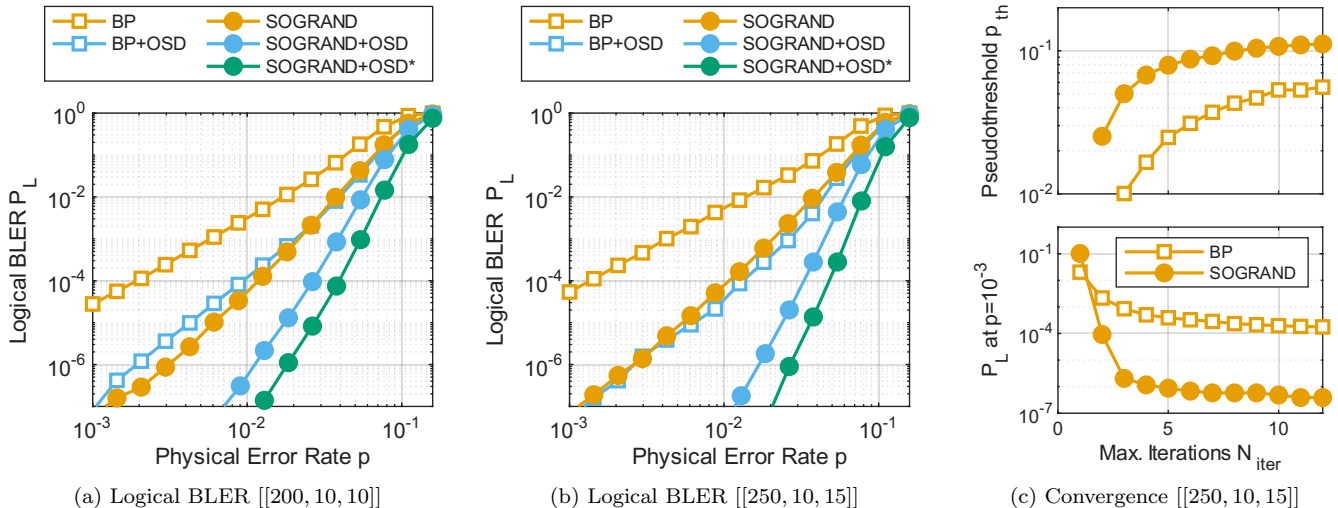


FIG. 2. Decoding performance for $[[250, 10, 15]]$ and $[[200, 10, 10]]$ quantum Tanner codes (a), (b) Logical block error rate (BLER) under depolarizing noise. SOGRAND decoding (circles) significantly outperforms standard BP (squares). The addition of OSD post-processing (blue) further suppresses errors, with the correlation-aware decoding *SOGRAND+OSD** (green) providing the best performance. (c) Convergence of the pseudothreshold p_{th} (top) and logical block error rate (BLER) at $p = 10^{-3}$ (bottom) as a function of the maximum decoding iterations N_{iter} .

$[[250, 10, 15]]$ introduced in Ref. [12]. Unlike Ref. [12], which flattens the Tanner construction into a global parity check matrix for standard BP, we extract the underlying Tanner code graphs and the (25, 19) component codes, and decode the Tanner codes as generalized LDPC codes directly with SOGRAND. We evaluate the decoder on a depolarizing channel with total physical error rate p , where each qubit undergoes an X , Y , and Z error with probability $p/3$. For independent X and Z decoding, we map the depolarizing channel to two independent binary symmetric channels with effective flip probability $\tilde{p} = 2/3p$ and set the initial LLR to $L_{ch,i} = \log((1 - \tilde{p})/\tilde{p})$. For the correlation aware variant, we initialize the beliefs to $P_{ch,i}^\mu = (1 - p)$ for $\mu = I$ and $P_{ch,i}^\mu = p/3$ otherwise.

Figures 2a and 2b summarize the decoding performance. As a baseline, we evaluate standard BP using the LDPCv2 package [48, 49] with min-sum decoding, a scaling factor $\alpha = 0.625$, and $N_{iter} = 100$. For SOGRAND, we set $N_{iter} = 20$. Both BP+OSD and SOGRAND+OSD use OSD-9 of the LDPCv2 package with combination strategy. SOGRAND+OSD, achieves a logical block error rate (BLER) of 10^{-7} at $p \approx 10^{-2}$, whereas BP+OSD requires $p = 10^{-3}$ to reach the same reliability. This demonstrates that even with OSD post-processing, BP provides suboptimal performance on these quantum Tanner code instances. Consequently, even without OSD, SOGRAND matches or exceeds the performance of BP+OSD. Furthermore, for the depolarizing channel, the correlation-aware variant (SOGRAND+OSD*) demonstrates that the SOGRAND framework can efficiently exploit noise correlation, further boosting perfor-

mance. This enhanced performance comes with minimal additional computational overhead.

This superior performance is achieved with remarkably few decoding iterations compared to BP. Figure 2c (bottom) quantifies this convergence speed and shows the logical BLER at $p = 10^{-3}$ for both BP and SOGRAND as a function of N_{iter} . Due to the stronger component codes, SOGRAND realizes the majority of its error correction gain within the first three decoding iterations, whereas BP converges more gradually. This advantage is reflected in the pseudo-threshold p_{th} , Fig. 2c (top), defined as the physical error rate at which the logical BLER of the n coded qubits equals that of k uncoded qubits, $1 - (1 - p)^k$. For small p , the BLER of k uncoded qubits is approximately k times the physical error rate, kp .

The primary bottleneck for real-time quantum error correction is algorithmic *depth*, i.e., the sequence of operations that must be performed serially owing to data dependencies. Because decoding iterations are inherently sequential, the total latency is the product of the iteration count and the depth per iteration. For SOGRAND decoding, the internal querying process is inherently parallelizable [41]. For the analyzed codes, which have 6 redundancy bits per component code, each candidate error pattern in \mathcal{L} is typically found in fewer than $2^6 = 64$ parallel queries. Because the local component codes have a fixed length [9], the algorithmic depth per iteration is independent of the codeword length n . By combining a low iteration count with the constant iteration depth, as demonstrated in Fig. 2c, SOGRAND-based decoding offers a scalable framework for low-latency quantum error correction.

Conclusion.—This work proposes SOGRAND decoding for quantum Tanner codes. Performance evaluation on explicit instances demonstrates that the proposed decoder, when combined with OSD post-processing, outperforms the established BP+OSD baseline by up to three orders of magnitude in logical BLER. Even without OSD post-processing, the SOGRAND-based decoder alone can match the performance of BP+OSD, effectively removing the cubic complexity bottleneck associated with OSD. This highlights the great potential of the quantum Tanner code class, as it admits a far more effective decoder. Since the approach relies on iterative message passing, existing optimization techniques for standard BP, such as neural belief propagation [50], can be readily adopted. Although presented within the code capacity setting [32], none of the presented techniques inherently rely on error-free syndrome measurements. Following similar extensions for BP [51], the noise model can be relaxed to phenomenological and circuit-level noise [32, 33]. Characterizing SOGRAND’s performance under these models is a promising direction for future work. These results suggest a viable path toward practical, scalable implementations of quantum Tanner codes.

Note.—During the completion of this manuscript, we became aware of concurrent research on the iterative decoding of quantum Tanner codes [52]. The primary distinction between these works is that Ref. [52] focuses broadly on decoding quantum codes with generalized LDPC structure, with quantum Tanner codes as a paradigmatic example, whereas our work centers on the use of SOGRAND as a highly effective SISO decoder. In Ref. [52], component code decoding is performed using an exact MAP decoder implemented via the BCJR algorithm. This provides an upper bound on the decoding performance, but is computationally inefficient. Indeed, Ref. [52] identifies the development of an efficient SISO decoding algorithm for the component codes as an open problem, which is resolved here using SOGRAND.

* rappl@mit.edu

† medard@mit.edu

‡ e.tang@northeastern.edu

§ k.duffy@northeastern.edu

- [1] A. Kitaev, *Annals of Physics* **303**, 2–30 (2003).
- [2] S. B. Bravyi and A. Y. Kitaev, Quantum codes on a lattice with boundary (1998), arXiv:quant-ph/9811052 [quant-ph].
- [3] D. MacKay, G. Mitchison, and P. McFadden, *IEEE Transactions on Information Theory* **50**, 2315–2330 (2004).
- [4] J.-P. Tillich and G. Zémor, *IEEE Trans. Inf. Theory* **60**, 1193 (2014).
- [5] N. P. Breuckmann and J. N. Eberhardt, *PRX Quantum* **2**, 10.1103/prxquantum.2.040101 (2021).
- [6] D. Gottesman, *Quantum Info. Comput.* **14**, 1338 (2014).
- [7] N. P. Breuckmann and J. N. Eberhardt, *IEEE Transactions on Information Theory* **67**, 6653–6674 (2021).
- [8] P. Panteleev and G. Kalachev, in *Proceedings of the 54th Annual ACM SIGACT Symposium on Theory of Computing* (ACM, New York, 2022) pp. 375–388.
- [9] A. Leverrier and G. Zémor, in *Proceedings of the 63rd Annual IEEE Symposium on Foundations of Computer Science* (New York, 2022) pp. 872–883.
- [10] A. Leverrier, W. Rozendaal, and G. Zémor, Small quantum Tanner codes from left-right Cayley complexes (2025), arXiv:2512.20532 [quant-ph].
- [11] V. Guémard and G. Zémor, Moderate-length lifted quantum Tanner codes (2025), arXiv:2502.20297 [quant-ph].
- [12] R. K. Radebold, S. D. Bartlett, and A. C. Doherty, Explicit instances of quantum Tanner codes (2025), arXiv:2508.05095 [quant-ph].
- [13] B. M. Terhal, *Rev. Mod. Phys.* **87**, 307 (2015).
- [14] R. G. Gallager, *Low-Density Parity-Check Codes*, Ph.D. thesis, MIT (1963).
- [15] Z. Babar, P. Botsinis, D. Alanis, S. X. Ng, and L. Hanzo, *IEEE Access* **3**, 2492 (2015).
- [16] D. Poulin and Y. Chung, *Quantum Info. Comput.* **8**, 987 (2008).
- [17] N. Raveendran and B. Vasić, *Quantum* **5**, 562 (2021).
- [18] P. Panteleev and G. Kalachev, *Quantum* **5**, 585 (2021).
- [19] J. Valls, F. Garcia-Herrero, N. Raveendran, and B. Vasić, *IEEE Access* **9**, 138734 (2021).
- [20] J. Boutros, O. Pothier, and G. Zémor, in *Proceedings of the IEEE International Conference on Communications* (IEEE, New York, 1999) pp. 441–445.
- [21] I. Dinur, M.-H. Hsieh, T.-C. Lin, and T. Vidick, in *Proceedings of the 55th Annual ACM Symposium on Theory of Computing*, STOC 2023 (Association for Computing Machinery, New York, NY, USA, 2023) p. 905–918.
- [22] S. Gu, C. A. Pattison, and E. Tang, in *Proceedings of the 55th Annual ACM Symposium on Theory of Computing*, STOC 2023 (Association for Computing Machinery, New York, NY, USA, 2023) p. 919–932.
- [23] A. Leverrier and G. Zémor, *IEEE Trans. Inf. Theory* **69**, 5100 (2023).
- [24] S. Gu, E. Tang, L. Caha, S. H. Choe, Z. He, and A. Kubica, *Commun. Math. Phys.* **405**, 85 (2024).
- [25] A. Leverrier and G. Zémor, *ACM Trans. Algorithms* **21**, 35 (2025).
- [26] P. Yuan, M. Médard, K. Galligan, and K. R. Duffy, *IEEE Trans. Wireless Commun.* **24**, 3386 (2025).
- [27] E. Kizilates, A. Riaz, A. Bali, J. Feng, M. Médard, K. R. Duffy, and R. T. Yazicigil, in *Proceedings of the IEEE Custom Integrated Circuits Conference* (IEEE, New York, 2026).
- [28] I. Dinur, S. Evra, R. Livne, A. Lubotzky, and S. Mozes, in *Proceedings of the 54th Annual ACM SIGACT Symposium on Theory of Computing* (ACM, New York, 2022) pp. 357–374.
- [29] O. Á. Mostad, E. Rosnes, and H.-Y. Lin, *IEEE J. Sel. Areas Inf. Theory* **6**, 367 (2025).
- [30] A. R. Calderbank and P. W. Shor, *Phys. Rev. A* **54**, 1098 (1996).
- [31] A. M. Steane, *Phys. Rev. Lett.* **77**, 793 (1996).
- [32] E. Dennis, A. Kitaev, A. Landahl, and J. Preskill, *J. Math. Phys.* **43**, 4452 (2002).
- [33] A. M. Stephens, *Phys. Rev. A* **89**, 022321 (2014).
- [34] R. Tanner, *IEEE Trans. Inf. Theory* **27**, 533 (1981).

- [35] K. R. Duffy, P. Yuan, J. Griffin, and M. Médard, *IEEE Commun. Lett.* **29**, 328 (2025).
- [36] P. Yuan, K. R. Duffy, and M. Médard, *IEEE Trans. Inf. Theory* **71**, 1007 (2025).
- [37] K. R. Duffy, J. Li, and M. Médard, *IEEE Trans. Inf. Theory* **65**, 4023 (2019).
- [38] D. Cruz, F. A. Monteiro, and B. C. Coutinho, *IEEE Access* **11**, 119446 (2023).
- [39] D. Chandra, Z. B. Kaykac Egilmez, Y. Xiong, S. X. Ng, R. G. Maunder, and L. Hanzo, *IEEE Access* **11**, 19059 (2023).
- [40] D. Cruz, F. A. Monteiro, A. Roque, and B. C. Coutinho, *IEEE Trans. Quantum Eng.* **6**, 1 (2025).
- [41] K. R. Duffy, W. An, and M. Médard, *IEEE Trans. Signal Process.* **70**, 4528 (2022).
- [42] K. R. Duffy, M. Grundei, and M. Médard, in *Proceedings of the IEEE Global Communications Conference* (IEEE, New York, 2023) pp. 3585–3590.
- [43] C. Condo, V. Bioglio, and I. Land, in *Proceedings of the IEEE Globecom Workshops* (IEEE, New York, 2021) pp. 1–6.
- [44] C. Condo, *IEEE Trans. Circuits Syst. I: Regul. Pap.* **69**, 2203 (2022).
- [45] S. M. Abbas, T. Tonnellier, F. Ercan, M. Jalaeddine, and W. J. Gross, *IEEE Trans. Very Large Scale Integr. (VLSI) Syst.* **30**, 681 (2022).
- [46] A. Riaz, A. Yasar, F. Ercan, W. An, J. Ngo, K. Galligan, M. Médard, K. R. Duffy, and R. Tugce Yazicigil, *IEEE J. Solid-State Circuits* **60**, 2645 (2025).
- [47] C.-Y. Lai and K.-Y. Kuo, *IEEE Trans. Quantum Eng.* **2**, 1 (2021).
- [48] J. Roffe, LDPC: Python tools for low density parity check codes (2022), <https://pypi.org/project/ldpc/>.
- [49] J. Roffe, D. R. White, S. Burton, and E. Campbell, *Phys. Rev. Res.* **2**, 043423 (2020).
- [50] Y.-H. Liu and D. Poulin, *Phys. Rev. Lett.* **122**, 200501 (2019).
- [51] K.-Y. Kuo and C.-Y. Lai, *IEEE Trans. Inf. Theory* **71**, 1824 (2025).
- [52] O. Å. Mostad, E. Rosnes, and H. Yin-Lin, Improved decoding of quantum tanner codes using generalized check nodes (2026), arXiv:2603.05486 [quant-ph].